



Selective Detection of Zn²⁺ Ions by Ratiometric Receptor (E)-N'-(1-(2, 5-Dihydroxy phenyl) Ethylidene) Isonicotinohydrazide: A DFT Study

N. S. Patil*(**), R. B. Dhake*, R. Phalak*, U. A. Fegade**† , C. Ramalingan*** and V. Saravanan***

*Department of Chemistry, D. D. N. Bhole College, Bhusawal, Jalgaon 425201, Maharashtra, India

**Department of Chemistry, Bhusawal Arts, Science and P. O. Nahata Commerce College, Bhusawal, Jalgaon 425201, Maharashtra, India

***Department of Chemistry, Kalasalingam Academy of Research and Education (Deemed to be University), Krishnankoil 626 126, Tamilnadu, India

†Corresponding author: U. A. Fegade; umeshfegade@gmail.com

Nat. Env. & Poll. Tech.
Website: www.neptjournal.com

Received: 21-05-2022
Revised: 26-06-2022
Accepted: 30-06-2022

Key Words:

Detection of zinc
Ratiometric receptor
Isonicotinohydrazide
DFT study

ABSTRACT

The metal ion sensing characteristics of a novel Schiff-based ratiometric UV-visible chemosensor (E)-N'-(1-(2,5-dihydroxy phenyl)ethylidene) isonicotinohydrazide (R1) has been explored. In EtOH:H₂O (7:3, v/v), it has high sensitivity and selectivity for Zn²⁺ among a series of metal ions. With the addition of Zn²⁺ ions solution, R1 displayed discriminating spectral activity. The other metal ions did not affect R1 in any way. Furthermore, the addition of Zn²⁺ ions to R1 and LMCT action caused the shifting of the peak to a longer wavelength of 406 nm. The interaction of Zn²⁺ ions with R1 was further investigated using Density Functional Theory (DFT) investigations. Zn²⁺-R1 combination has a lower energy (2.2667 kcal.mol⁻¹ to 0.9339 kcal.mol⁻¹) than R1, indicating a strong connection with excellent stability. The Zn²⁺-R1 complex's association constant (K_a) was discovered to be 6795M⁻¹ and 6836M⁻¹ using Benesi-Hildebrand and Scatchard plots respectively. The detection limit was determined to be 276 nM.

INTRODUCTION

Many industrial processes rely heavily on transition metals including iron, zinc, and nickel. For the production of ammonia and fertilizers, iron is employed as a catalyst. Nickel is a key component of various steel-based alloys due to its high strength and resilience to corrosion and heat in the steel industry. Galvanization of iron is generally done with zinc. In the paint and dye-based industries, iron and zinc oxides are extensively employed as pigments (Lehn 1995, Atood et al. 1996).

Zinc is often seen securely bound in proteins in the human body. It plays a range of vital roles in biological processes. Infantile diarrhea, Parkinson's disease, and Alzheimer's disease, immunological dysfunction might all be caused by a disturbance of Zn(II) homeostasis (Lehn 1995, Atood et al. 1996, De Silva et al. 1997, Kumar et al. 2018, An et al.

2016). As a result, creating probes that can properly detect and understand in vivo Zn(II) biological processes requires the ability to observe Zn(II) concentration in biological systems.

Because of their importance in a range of biological and industrial processes, effective real-time atomic detection of all of these metals is critical. For detecting them, several analytical approaches are available (Zhang et al. 2019a, 2020, Khanna et al. 2019, Ghorai et al. 2019, Yan et al. 2018, Dong et al. 2017). Metal sensing based on optical phenomena is a growing subject of study (Fegade et al. 2014a). Because of its simplicity, ease of use, real-time detection, cheap cost, excellent selectivity, and sensitivity, in the environmental, analytical, and biological realms, this technique has a wide range of applications (Fegade et al. 2014b, 2015a, 2015b, Patil et al. 2014, Kuwar et al. 2013, Tayade et al. 2014, Pawar et al. 2015, Patil et al. 2015, 2014, 2020, Bhosale et al. 2015, Kaur et al. 2017, Kolate et al. 2020, Fegade et al. 2021a, 2021b).

In comparison to fluorescence-based chemosensors, other detection techniques such as AAS, XRF, radioisotopes, ICP-MS (Berrones-Reyes et al. 2019), modified nanotube carbon

 ORCID details of the authors:

Umesh Fegade:

<https://orcid.org/0000-0002-2599-668X>

electrodes (Khanra et al. 2019), voltammetry (Zhang et al. 2019b), and ion-selective membrane electrodes (Diana et al. 2019, Jung et al. 2019) have a substantial benefit. Fluorescent chemosensors are appealing approaches because of their low cost, high selectivity, sensitivity, and ability to detect in real-time (Ghorai et al. 2019, Yan et al. 2018, Dong et al. 2017, Fegade et al. 2014c, Fegade et al. 2015a, 2015b, Patil et al. 2014,). Chemosensors have played a significant role in gaining a better knowledge of biological processes and their applications in the environment. In recent years, chromogenic zinc sensing molecules have been extensively produced for the goal of monitoring and/or detecting the transient and dynamic distribution of zinc ions inside the cell (Fegade et al. 2014d, 2015a, 2015b, 2020, 2021a, 2021b, Patil et al. 2014, 2015, 2021, Jethave et al. 2018, 2019, 2021, Xu et al. 2018, Yan et al. 2018).

Many transition metals are required for the chemistry of biological systems, with Fe, Co, Cu, and Mo being the most prevalent examples. However, because of the severe toxic consequences, simple, sensitive, selective, and Reliable sensing systems or sensors are required for detecting and eliminating metals from diverse environmental matrices (Lehn 1995, Atood et al. 1996, De Silva et al. 1997, Khan et al. 2013). However, these procedures have significant disadvantages, including a time-consuming sample preparation process, expensive costs, and the need for specialized instrumentation. Furthermore, due to the color change effect visible to the naked eye, identifying trace elements with a colorimetric probe is simple. The response time between the analyte and the probe is relatively short, and apparent color changes allow detection to move from the lab to on-site applications (An et al. 2016, Maniyazagan et al. 2017, Dong et al. 2017, Ghosh et al. 2017, Yang et al. 2019, Naha et al. 2020). In Schiff UV-visible/fluorescent probes, with metal ions, the C=N bond results in the formation of a stable complex., demonstrating the discriminating spectral activity. As a result, Schiff base probes have attracted the attention of several scientists in the fields of environmental and chemical sciences (Penden et al. 2019).

For a few years, our team has been working on detecting and removing organic and inorganic contaminants from the environment (Fegade et al. 2014e, 2015a, 2015b, 2020, 2021a, 2021b, Patil et al. 2014, 2015, 2021, Jethave et al. 2018, 2019, 2021). In this study, (E)-N'-(1-(2,5-dihydroxyphenyl) ethylidene) isonicotinohydrazide (R1) a Schiff base, was produced and tested in fluorescence and UV-visible spectrophotometers for the detection of Zn²⁺ ions. Color shift was observed by the human eye and wavelength enhancement and the shift was examined for the validation of Zn²⁺ interaction with the R1.

MATERIALS AND METHODS

Fisher Scientific Chemicals Ltd. in India provided all reagents, which were utilized without being purified further. The "1H NMR" spectra were acquired on a "Bruker Avance II 400 NMR" operating at 400 MHz in DMSO. The MASS and IR spectra were generated using water "QTOF-Q micro mass" and "Bruker FTIR spectrometers", respectively. A Shimadzu UV-1800 model with 1 cm quartz cells was used to perform the UV-visible spectrophotometric examination.

Synthesis of R1

A solution of isoniazide (0.411 g, 3 mmol) and 2,5-dihydroxy benzaldehyde (0.414 g, 3 mmol) are mixed in 50 mL of CH₃OH and provided 2 h of stirring at room temperature results in the yellow precipitate, which was purified, dehydrated, and recrystallized from ethanol (85%) to yield pure R1 (Fig. 1).

Photographic and Physical Examination

UV-visible spectrophotometer was used for the analysis of working solution R1 to assess metal ion selectivity, then various metal ions were added. R1 demonstrated a discriminating spectrum shift when Zn²⁺ ions were added, but other metal ions did not, resulting in photometric titrations.

DFT Research

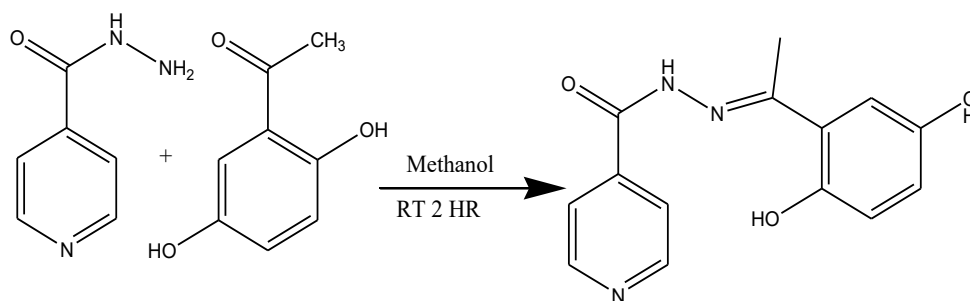


Fig. 1: Synthesis of R1.

GAUSSIAN 09 software was applied for all computational calculations. The optimal research was conducted at the B3LYP level, utilizing the Gaussian 09 program's 6-311G** basis set (for Zn atom). To establish the nature of the reaction, LUMO and HOMO values were used to monitor the interaction of Zn^{2+} ions with R1.

Calculation of the LOD

The detection limit was calculated using the equation below.

$$\text{LOD (limit of detection)} = 3/S$$

$$S = \text{Slope.}$$

RESULTS AND DISCUSSION

Chemosensor R1 was made by condensation reaction between isoniazide and 2,5-dihydroxy benzaldehyde in methanol (Fig. 1) and analyzed using Spectro-analytical methods. The purity of the R1 has been established based on IR, $^1\text{H-NMR}$, and mass spectroscopic techniques. $^1\text{H-NMR}$

(CDCl_3 , 400 MHz, ppm, δ): 2.43 (s, 3H, CH_3), 6.72-6.79 (m, 2H, Ar-H), 6.980 (s, 1H, Ar-H), 7.82-7.83 (m, 2H, Ar-H), 8.76-8.77 (m, 2H, Ar-H), 8.84 (s, 1H, -OH), 11.49 (s, 1H, -NH), 12.436 (s, 1H, -NH), IR (KBr, cm^{-1}) $\nu = 668.34$, 752.60, 781.20, 831.42, 1149.44, 1208.93, 1292.38, 1504.27, 1533.90, 1665.88, 3452.81, MS (EI): $m/z = 271.0957$ ($\text{C}_{14}\text{H}_{13}\text{N}_3\text{O}_3$) calcd $m/z = 272.55163$ for $\text{C}_{14}\text{H}_{13}\text{N}_3\text{O}_3$ [39-43].

The behavior of R1 ($C = 1 \times 10^{-5}$ M) absorption in the presence of different metal ions ($C = 1 \times 10^{-4}$ M) was investigated using UV-visible spectrophotometric measurements. R1's UV-Visible spectra revealed two peaks at 396 nm, with $n \rightarrow \pi^*$ transitions ascribed to the peak. In addition, the addition of Zn^{2+} ion solution to R1 produced a ratiometric spectrum pattern, but the insertion of different ionic species had no effect. Because of the LMCT action, the addition of Zn^{2+} ion solution to R1 resulted in a red shift of the 396 nm peak to 406 nm, as seen in Fig.2a. The complex bond form between Zn^{2+} , OH of R1, and $\text{C}=\text{N}$ was identified. The redshift is generated by the -OH group being deprotonated,

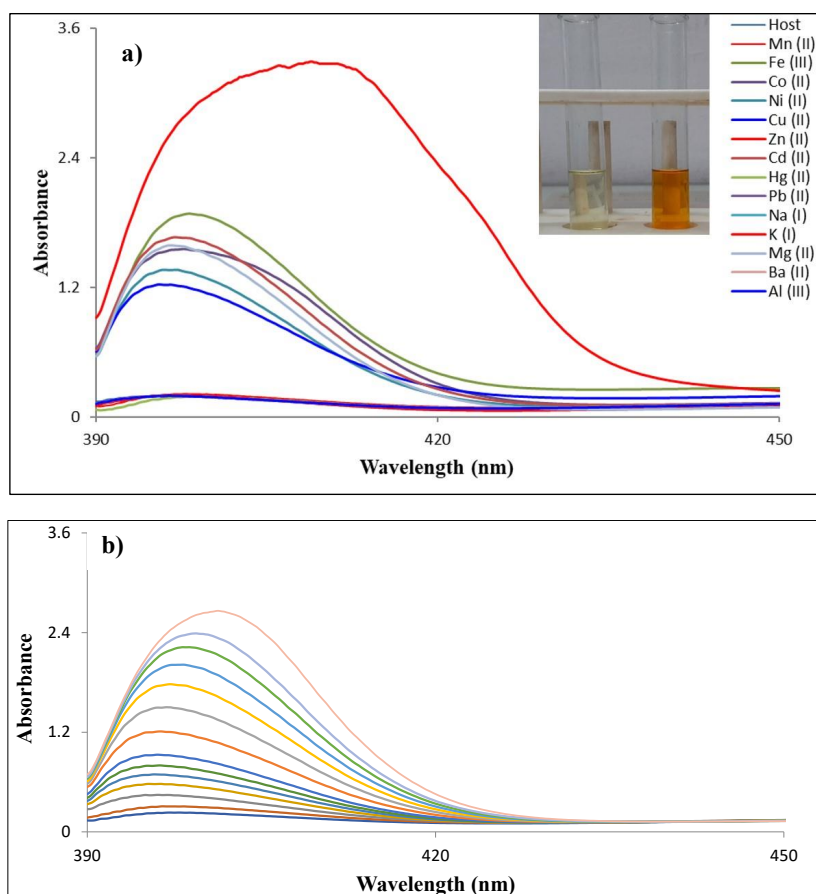


Fig. 2: a) Metal ion selectivity utilizing R1, Inset Fig. 2a Colour change of R1 (Pale yellow) with the addition Zn^{2+} (Orange) and b) R1 absorption profile with gradual addition of Zn^{2+} ion.

which leads to the formation of an O-Zn covalent bond. The addition of Zn^{2+} to R1 results in not only spectral shifts but there are also chromatic changes from yellow to orange, as measured by colorimetry. The color shift is visible with the naked eye (Fig. 2a Inset), increasing R1 efficiency in today's industrially polluted world (Benesi & Hildebrand 1949, Scatchard 1949, Xu et al. 2018).

Titrations were performed to have a better grasp of occurrence. The spectra of R1 were initially recorded, as shown in Fig. 1b, and then a Zn^{2+} ion solution varying in concentration from 0 to 200 μ L was introduced to R1 (2 mL). The absorbance at 396 nm increases as the amount of Zn^{2+} ions increase, allowing Zn^{2+} ions to be detected in both synthetic and actual samples. The absorption ratiometric response of R1 with Zn^{2+} in the presence of different metal

ions was investigated to evaluate selectivity, as shown in Fig. 3a. The interference study is crucial in the detection of target analytes because interfering ions have a major impact on the method's detection capabilities as well as the detection limit (Fig. 3b).

In the FTIR spectra of pure ligand, broadbands were seen at 3423 cm^{-1} and 3095 cm^{-1} , which correspond to the -OH and -NH stretching frequencies, respectively. Carbonyl and imine stretching frequency characteristic bands formed sharply at 1668 cm^{-1} and 1525 cm^{-1} , respectively. In the FTIR spectra of the equivalent R1- Zn^{2+} complex, the unique bands associated with -OH and -NH are diminished/decreased, and the band for carbonyl and imine stretching is moved to a lower wavelength in the complex at 1664 cm^{-1} and 1517 cm^{-1} , respectively (Yan et al. 2018, Meng et al.

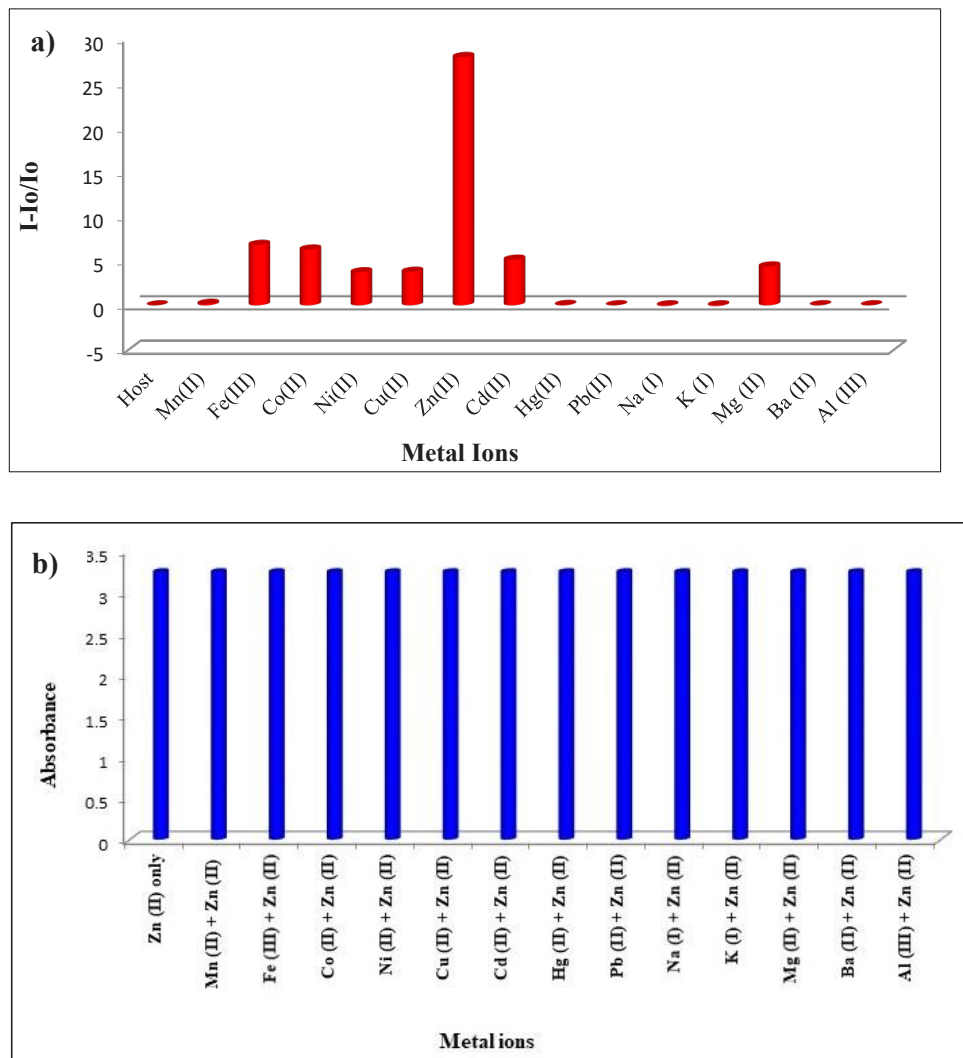


Fig. 3: a) Ratiometric graph of R1 with other metals and b) R1 interference investigations with Zn^{2+} in the existence of some of the other metal cations.

2018). For the imidol structure to become the dominant one during complexation, the ligand's amide functionality must have undergone amido-imidol tautomerism, according to the preceding facts. The band for the carbonyl and imine functional groups also shifts to a lesser wavelength due to the participation of N in the C=N with the Zn. $m.z^{-1} = 335.6534$ ($C_{14}H_{12}N_3O_3Zn$) calcd $m.z^{-1} = 336.0901$ for ($C_{21}H_{18}ClCuN_4O_2$).

The highest occupied MO and lowest unoccupied MO energy levels of the title sensor ligand R1 and the corresponding sensor ligand R1+Zn²⁺ are calculated computationally at the B3LYP level using the basis function system 6-311++G(d,p) to realize the impact of Zn²⁺ binding with the sensor ligand R1 and its electronic properties. 3D plots of the highest occupied MO and lowest unoccupied MO are furnished in Fig. 4 and the energy values are depicted in Table 1. The calculated highest occupied MO and lowest unoccupied MO energies of the sensor ligand R1 are -6.3356 eV and -4.0689 eV, respectively and the resulting bandgap energy (ΔE) of the sensor ligand R1 is 2.2667 eV. Alike, in the sensor ligand R1+Zn²⁺, the HOMO has an

energy of -4.3732 eV, whereas the LUMO has an energy of -3.4393 eV, and the bandgap energy is 0.9339 eV. As can be seen from the figure, the electron density in the highest occupied MOs of sensor ligand R1 is mainly confined to the dihydroxyphenyl structural motif while electron density in the lowest unoccupied MOs of the same is chiefly occupied on the pyridinyl scaffold. Besides, the density of electrons in the highest occupied MOs of sensor ligand R1+Zn²⁺ is primarily located on the dihydroxyphenyl unit akin to the pure sensor ligand R1, however, the density of electrons in the lowest unoccupied MOs of the same is positioned predominantly on the metal and its surroundings such as imine, carbonyl and one of the hydroxyl moieties coordinated with the metal. Precisely, when the highest occupied MOs and lowest unoccupied MOs are concerned, the predominant electron distribution region transfers from one province to another in both cases (Gangatharan et al. 2018, Khanra et al. 2019). On comparing the highest occupied MOs and the lowest unoccupied MOs energy difference between the sensor ligand R1+Zn²⁺ and the sensor ligand R1, the former has a lower value when compared to the latter reflecting the higher stability of the

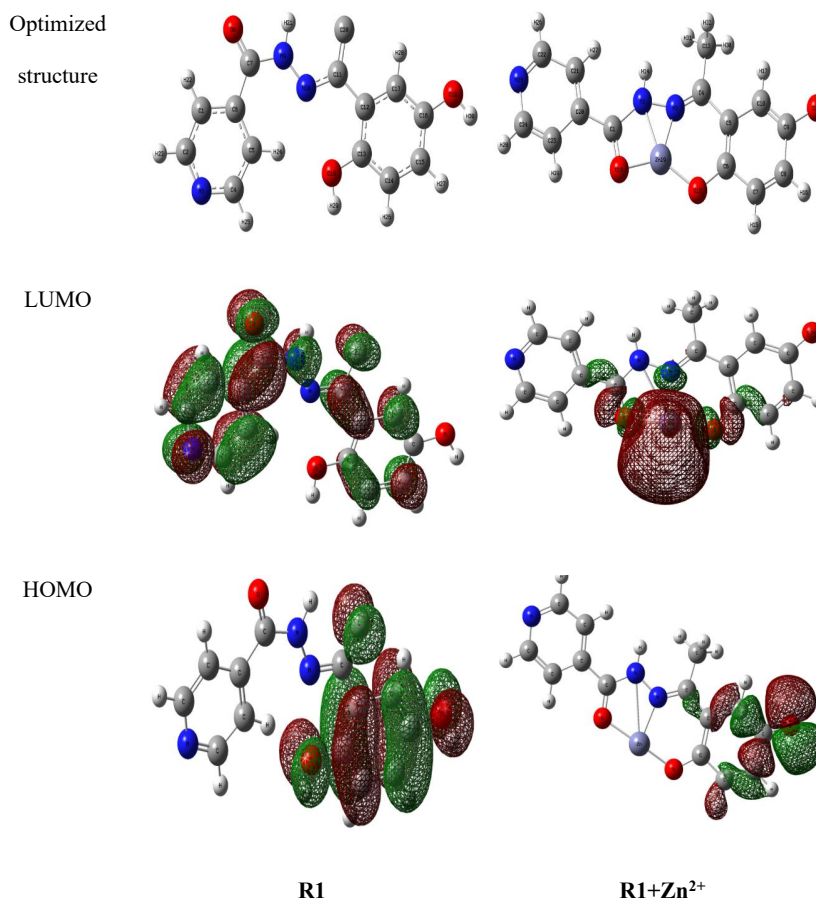


Fig. 4: DFT calculation (a) R1 and R1. Zn²⁺, (b) LUMO, (c) HOMO diagrams.

Table 1: Energies value of S1 and Sensor 3+Zn²⁺

Parameter	Energies (eV)	
	R1	R1+Zn ²⁺
HOMO	-6.3356	-4.3732
LUMO	-4.0689	-3.4393
ΔE	2.2667	0.9339

sensor ligand R1+Zn²⁺. Consequently, the results obtained from computational calculations are in good harmony with

the experimental analysis of the Zn²⁺ binding (Ghorai et al. 2019, Zhang et al. 2019a, 2019b, Awad et al. 2019).

The complex's binding constant may also be calculated by titrating R1 with a Zn²⁺ ion solution. Using Benesi-Hildebrand and Scatchard plots, the association constant (K_a) of the Zn²⁺-R1 complex was determined to be 6795M⁻¹ and 6836M⁻¹, respectively (Fig. 5a and 5b). As seen in Fig. 6, the binding stoichiometry is a constantly fluctuating process. The absorbance of the host H/([H]+[G]) was also shown in Fig. 6 for a range of total concentrations (Berrones-Reyes

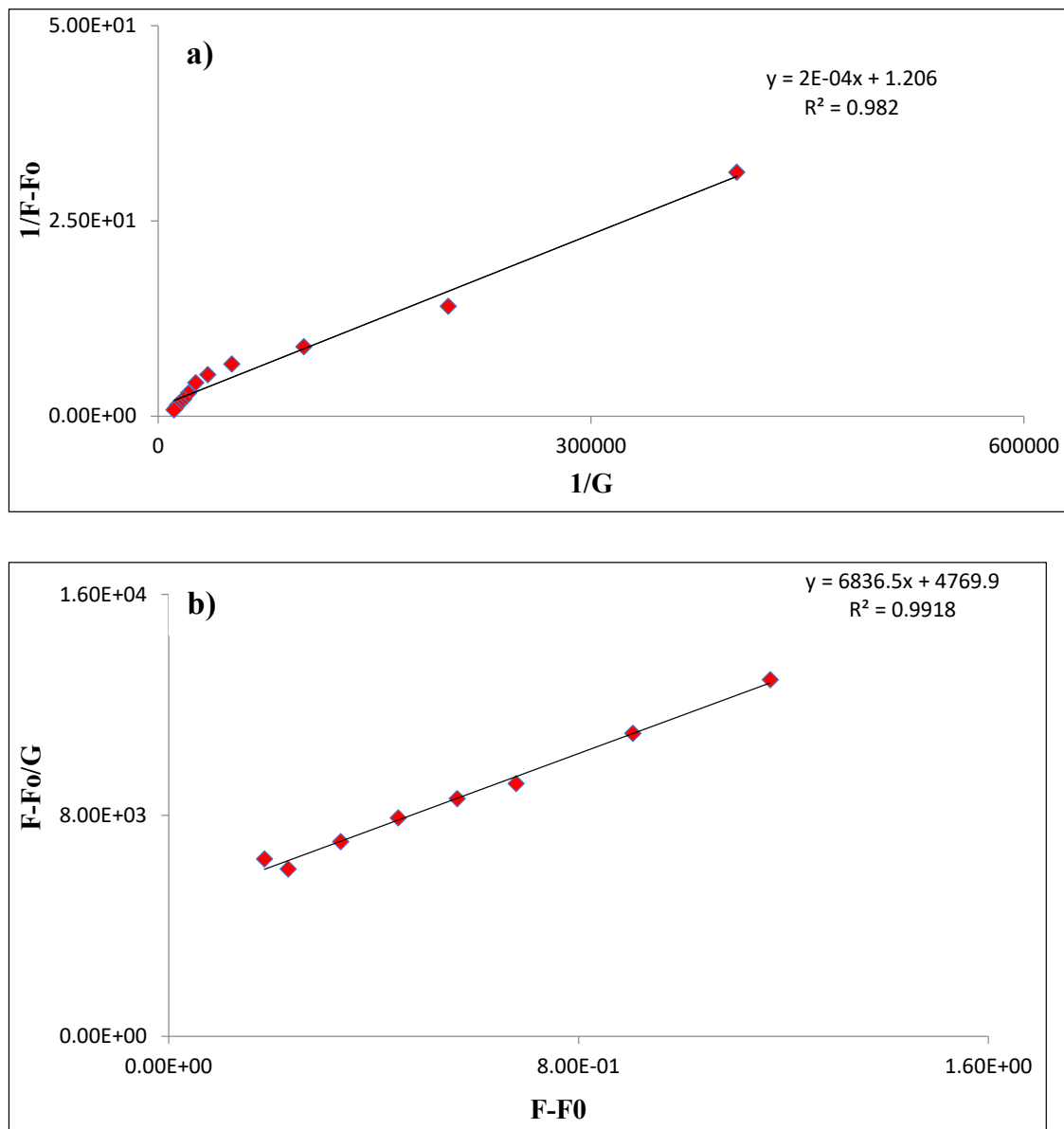


Fig. 5: a) Benesi-Hildebrand for R1 where the K_a value at 6795M⁻¹ and $R^2 = 0.982$, and b) Scatchard graph for R1 where the K_a value at 6836 M⁻¹ and $R^2 = 0.9981$.

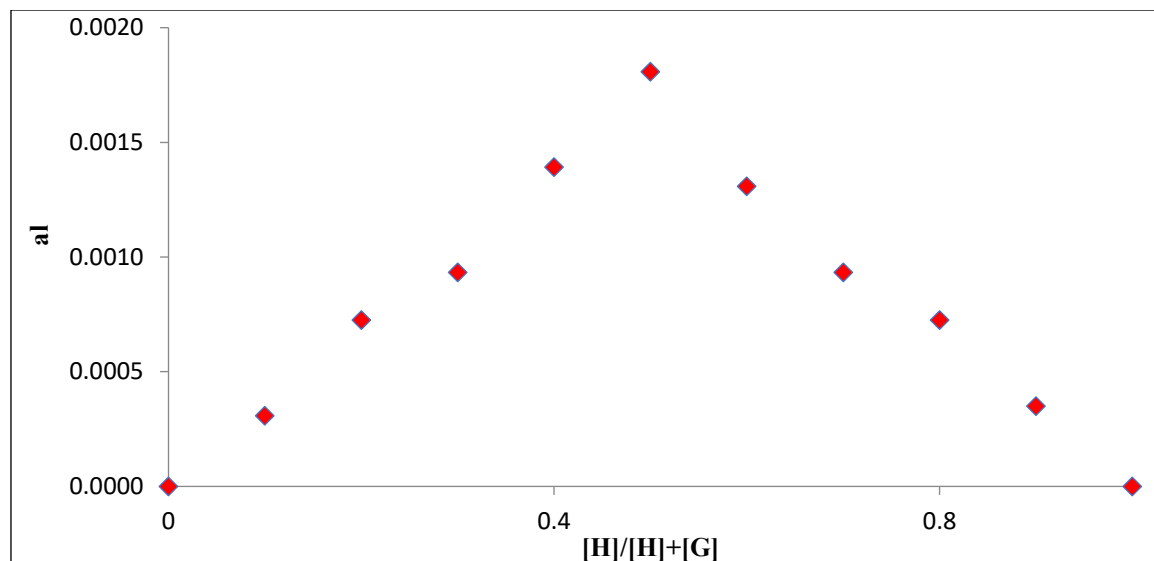


Fig. 6: Job plot between R1 and Zn^{2+} showing 1:1 complexation.

et al. 2019). The concentration of Zn^{2+} and R1 complex was found to be at a maximum of 0.5 units in Fig. 6. 276 nM detection limit (LOD) was found for the 1:1 stoichiometry of Zn^{2+} and R1 (Panunzi et al. 2019).

Reversibility and Colorimetrically Naked Eye Detection

Using absorption spectra, many ions were employed to investigate the reversible binding of Zn^{2+} ions. The brown hue of the Zn^{2+} -R1 was only removed with the addition of $EDTA^{2-}$. It's easy to see how the addition of $EDTA^{2-}$ may shatter the Zn^{2+} -R1 combination. The reversible reagent $EDTA^{2-}$ is used

to demetallize the compound and restore R1 to its natural color. Fig. 7 shows that R1 has greater reversibility of 6 cycles. The resulting complex was extracted with the $EDTA^{2-}$ after the Zn^{2+} ion sensing technique. In comparison to the published sensors (Li et al. 2019, Gu et al. 2019, Xu et al. 2019, Zhang et al. 2019a, 2019b), the regenerated R1 may be used numerous times to better detect Zn^{2+} ions, signifying sensitivity and cost-effectiveness. With the recommended colorimetric R1, the color shift from pale yellow to orange (Fig. 8) may be seen with the naked eye, as a consequence of this a reliable and selective sensor system for in-situ applications was designed (Mao et al. 2013, Guan et al. 2019, Park et al. 2014).

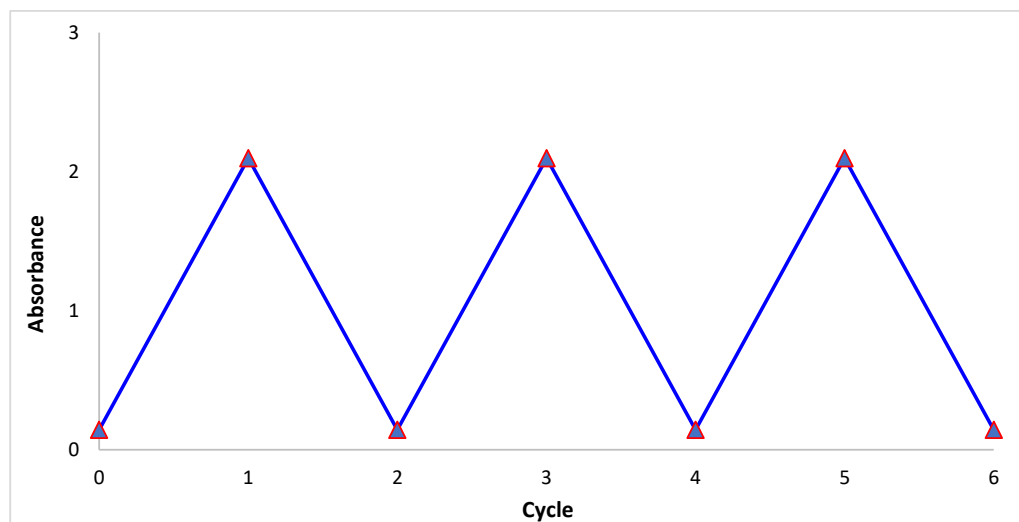


Fig. 7: A Receptor 1 reversible cycle with Zn^{2+} and $EDTA^{2-}$

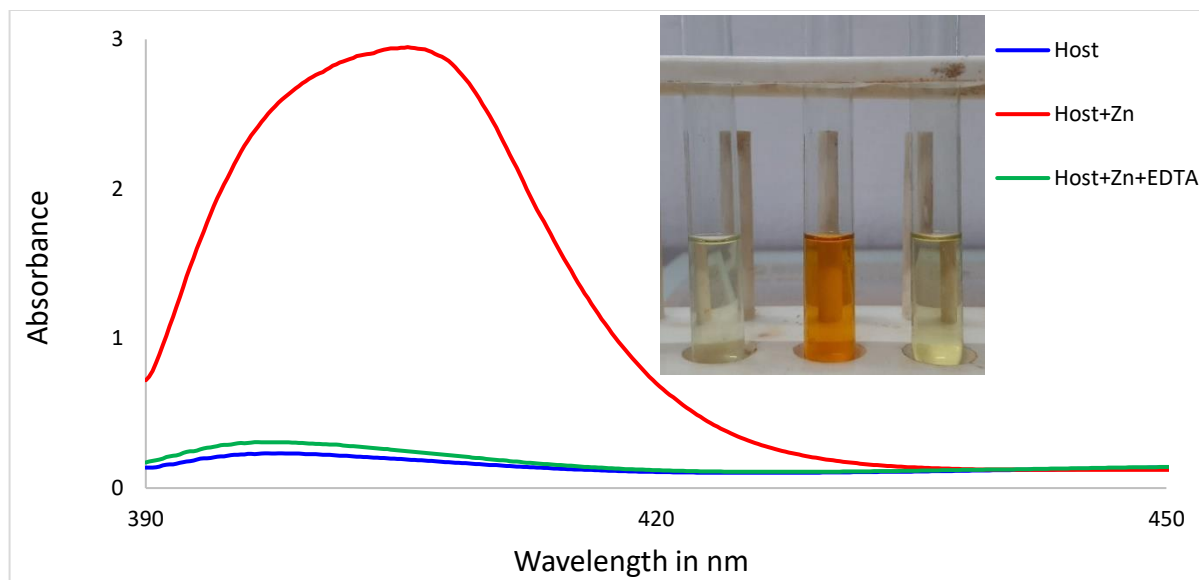


Fig. 8: a) Reversible cycle of R1 with Zn^{2+} and $EDTA^{2-}$, and b) graph of the reversible study, Inset figure capture of reversibility (R1, R1+Zn and R1+Zn+ EDTA).

ANALYTICAL APPLICATIONS

Recovery tests with real samples were done to assess the proposed colorimetric probe's selectivity, sensitivity, and reliability. Tap water and Mineral samples were taken from the industrial region of Bhusawal, Maharashtra, for the recovery tests. Zn^{2+} ions solutions with concentrations ranging from 10 to 25 $g.L^{-1}$ were introduced into the water samples. Table 2 showed that utilizing R1 resulted in better Zn^{2+} recoveries (> 97%) and lower percentage relative standard deviation (percent RSD) values (Cox et al. 2019, Bagheri et al. 2020, Zhou et al. 2014, Yang et al. 2019, Pendin et al. 2019, Yang 2019, Huang et al. 2019, Swami et al. 2018, Sargenti et al. 2014, Zhao et al. 2015, Kang et al. 2013).

CONCLUSIONS

Chemosensor R1 was made by condensation reaction between isoniazide and 2,5-dihydroxy benzaldehyde in

methanol and analyzed using Spectro-analytical methods. The UV-Visible spectra of R1 revealed two peaks 396nm and $n \rightarrow \pi^*$ 396 nm transitions are assigned to the peak. In addition, the addition of Zn^{2+} ion solution to R1 produced a ratiometric spectrum pattern, other metal ions, however, had no effect. Because of the LMCT action, the addition of Zn^{2+} ion solution to R1 resulted in a red shift of the 396nm peak to 406 nm. The Zn^{2+} -R1 complex's association constant (K_a) was discovered to be $6795M^{-1}$ and $6836M^{-1}$ using Benesi-Hildebrand and Scatchard plots respectively. The 1:1 stoichiometry of Zn^{2+} and R1 having a detection limit (LOD) of 276 nM.

REFERENCES

- An, R., Zhang, D., Chen, Y. and Cui, Y.Z. 2016. A "turn-on" fluorescent and a colorimetric sensor for selective detection of Cu^{2+} in aqueous media and living cells. *Sensors Actuat. B Chem.*, 222: 48-54.
 Atood, J., Davies, J., MacNicol, D. and Vogette, F. 1996. *Comprehensive Supramolecular Chemistry*. Elsevier Exeter, The Netherlands.

Table 2: Results of a Real sample of Zn^{2+} sensing

Sample	Zn^{2+} added ($\mu g.L^{-1}$)	Zn^{2+} found ($\mu g.L^{-1}$) using R1	Recovery (%) by R1 (n=3)
Mineral water	10	9.86 ± 0.045	99.01
	15	13.99 ± 0.084	99.24
	25	24.72 ± 0.053	99.32
Tap water	10	9.89 ± 0.049	98.42
	15	14.71 ± 0.047	98.61
	25	24.71 ± 0.037	98.88

N = Number of samples.

- Awad, I., Said, Nikolai I. Georgiev, Vladimir B. and Bojinov, A. 2019. Smart chemosensor: Discriminative multi-detection and various logic operations in aqueous solution at biological pH. *Spectrochim. Acta A Mol. Biomol. Spectrosc.*, 223: 117304.
- Bagheri, M. and Masoomi, M.Y. 2020. Sensitive ratiometric fluorescent metal-organic framework sensor for calcium signaling in human blood ionic concentration media. *ACS Appl. Mater. Interfaces*, 12(4): 4625-4631.
- Benesi, H.A. and Hildebrand, J.H.J. 1949. A spectrophotometric investigation of the interaction of iodine with aromatic hydrocarbons. *J. Am. Chem. Soc.*, 71(8): 2703-2707.
- Berrones-Reyes, J.C., Muñoz-Flores, B.M., Cantón-Díaz, A.M., Treto-Suárez, M.A., Páez-Hernández, D., Schott, E., Zarate, X. and Jiménez-Pérez, V.M. 2019. Quantum chemical elucidation of the turn-on luminescence mechanism in two new Schiff bases as selective chemosensors of Zn²⁺: Synthesis, theory and bioimaging applications. *RSC Adv.*, 9(53): 30778-30789.
- Bhosale, J., Fegade, U., Bondhopadhyay, B., Kaur, S., Singh, N., Basu, A., Dabur, R., Bendre, R. and Kuwar, A. 2015. Pyrrole-coupled salicylimine-based fluorescence "turn on" probe for highly selective recognition of Zn²⁺ ions in mixed aqueous media: Application in living cell imaging. *J. Mol. Recog.*, 28(6): 369-375.
- Cox, R.P., Sandanayake, S., Scarborough, D.L.A., Izgorodina, E.I., Langford, S.J. and Bell, T.D.M. 2019. Investigation of cation binding and sensing by new crown ether substituted naphthalene diimide systems. *New J. Chem.*, 43(4): 2011-2018.
- De Silva, A.P., Gunaratne, H.N., Gunnlaugsson, T., Huxley, A.J., McCoy, C.P., Rademacher, J.T. and Rice, T.E. 1997. Signaling recognition events with fluorescent sensors and switches. *Chem. Rev.*, 97(5): 1515-1566.
- Diana, R., Panunzi, B., Tuzi, A., Piotto, S., Concilio, S., Caruso, U. 2019. An amphiphilic pyridinoyl-hydrazone probe for colorimetric and fluorescence pH sensing. *Molecules* 24(21): 3833-3855.
- Dong, W.K., Akogun, S.F., Zhang, Y., Sun, Y.X. and Dong, X.Y. 2017. A reversible "turn-on" fluorescent sensor for selective detection of Zn²⁺. *Sensors Actuat. B Chem.*, 238: 723-734.
- Fegade, U., Bhosale, J., Sharma, H., Singh, N., Bendre, R. and Kuwar, A. 2015a. Fluorescence chemosensor for HSO₄⁻ ion based on pyrrole-substituted salicylimine Zn²⁺ complex: Nanomolar detection. *J. Fluoresc.*, 25(4): 819-824.
- Fegade, U., Jethave, G., Attarde, S., Kolate, S., Inamuddin, Altalhi, T. and Kanchi, S. 2021a. statistical physics model of EBT adsorption on Pb (II) doped zinc oxide nanoparticles: Kinetics, isotherm and reuse study. *Int. J. Environ. Anal. Chem.*, 16: 1-15.
- Fegade, U., Jethave, G., Hong, W.G., Khan, I., Marwani, H.M., Wu, R.J. and Dhake, R. 2020. Multifunctional Zn_{0.3}Al_{0.4}O_{4.5} crystals: An efficient photocatalyst for formaldehyde degradation and EBT adsorption. *Arab. J. Chem.*, 13(11): 8262-8270.
- Fegade, U., Kolate, S., Gokulakrishnan, K., Ramalingan, C., Altalhi, T. and Kanchi, S. 2021b. A selective ratiometric receptor 2-((E)-(3-(prop-1-en-2-yl)phenylamino) methyl)-4-nitrophenol for the detection of Cu²⁺ ions supported by DFT studies. *J. Fluoresc.*, 31(3): 625-634.
- Fegade, U., Patil, S., Kaur, R., Sahoo, S.K., Singh, N., Bendre, R. and Kuwar, A. 2015b. A novel chromogenic and fluorogenic chemosensor for the detection of trace water in methanol. *Sensors Actuat. B. Chem.*, 210: 324-327.
- Fegade, U., Sahoo, S.K., Singh, A., Mahulikar, P., Attarde, S., Singh, N. and Kuwar, A. 2014a. A selective and discriminating noncyclic receptor for HSO₄⁻ ion recognition. *RSC Adv.*, 4(29): 15288-15292
- Fegade, U., Saini, A., Sahoo, S.K., Singh, N., Bendre, R. and Kuwar, A. 2014b. 2, 2'-((Hydrazine-1, 2-diylidenedimethylidene) bis (6-isopropyl-3-methylphenol) based selective dual-channel chemosensor for Cu²⁺ in semi-aqueous media. *RSC Adv.*, 4(75): 39639-39644.
- Fegade, U., Sharma, H., Singh, N., Ingle, S., Attarde, S. and Kuwar, A. 2014c. An amide-based dipodal Zn²⁺ complex for multinationals recognition: Nanomolar detection. *J. Luminesc.*, 149: 190-195.
- Fegade, U., Singh, A., Chaitanya, G.K., Singh, N., Attarde, S. and Kuwar, A. 2014d. Highly selective and sensitive receptor for Fe³⁺ probing. *Spectrochim. Acta Part A Mol. Biomol. Spectrosc.*, 121: 569-574.
- Fegade, U., Tayade, S., Chaitanya, G.K., Attarde, S. and Kuwar, A. 2014e. Fluorescent and chromogenic receptor bearing amine and hydroxyl functionality for iron (III) detection in aqueous solution. *J. Fluoresc.*, 24(3): 675-681.
- Gangatharan, Vinoth Kumar Gujuluva, Kesavan Mookkandi Palsamy, Sivaraman Gandhi, Annaraj Jamespandi, Anitha Kandasamy, Tamilselvi Arunachalam, Athimoolam Shenmuganarayanan, Sridhar Balasubramaniam, and Rajesh Jegathalaprathaban. 2018. Reversible NIR fluorescent probes for Cu²⁺ ions detection and its living cell imaging. *Sensors and Actuators B: Chemical*, 255: 3235-3247.
- Ghorai, P., Banerjee, S., Nag, D., Mukhopadhyay, S.K. and Saha, A. 2019. Design and synthesis of a novel fluorescent-colorimetric chemosensor for selective detection of Zn (II) and Cu (II) ions with applications in live cell imaging and molecular logic gate. *J. Luminesc.*, 205: 197-209.
- Ghosh, U., Bag, S.S. and Mukherjee, C. 2017. Bis-pyridobenzene as a fluorescence light-up sensor for Hg²⁺ Ion in water. *Sensors Actuat. B. Chem.*, 238: 903-907.
- Gu, Y.Q., Shen, W.Y., Mi, Y., Jing, Y.F., Yuan, J.M., Yu, P., Zhu, X.M. and Hu, F.L. 2019. Dual-response detection of Ni²⁺ and Cu²⁺ ions by a pyrazolopyrimidine-based fluorescent sensor and the application of this sensor in bioimaging. *RSC Adv.*, 9(61): 35671-35676.
- Guan, J., Tu, Q., Chen, L., Yuan, M.S. and Wang, J. 2019. A benzothiazole-rhodol based luminophore: ESIPT-induced AIE and an application for detecting Fe²⁺ ion. *Spectrochim. Acta Part A Mol. Biomol. Spectrosc.*, 220: 117114.
- Huang, M.X., Lv, C.H., Huang, Q.D., Lai, J.P. and Sun, H. 2019. A novel and fast responsive turn-on fluorescent probe for the highly selective detection of Cd²⁺ based on photo-induced electron transfer. *RSC Adv.*, 9(62): 36011-36019.
- Jung, J.M., Yun, D., Lee, H., Kim, K. and Kim, C. 2019. Selective chemosensor capable of sensing both CN⁻ and Zn²⁺: Its application to zebrafish. *Sensors Actuat. B Chem.*, 297: 126814
- Jethave, G. and Fegade, U. 2018. Design and synthesis of Zn_{0.3}Fe_{0.45}O₃ nanoparticle for efficient removal of congo red dye and its kinetic and isotherm investigation. *Int. J. Ind. Chem.*, 9(1): 85-97.
- Jethave, G., Attarde, S., Fegade, U., Altalhi, T., Kanchi, S., Ingle, S. and Dhake, R. 2021. Statistical modeling and interpretation of sono-assisted adsorption mechanism of crystal violet dye on FeTiPbO nanocomposite. *J. Mol. Liq.*, 340: 116878.
- Jethave, G., Fegade, U., Attarde, S. and Ingle, S. 2019. Decontamination study of eriochrome Black-T from wastewater by using AlTiPbO nanoparticles (ATPO-NPs) for a sustainable clean environment. *J. Water Environ. Nanotechnol.*, 4: 263-274.
- Kang, J., Kang, H.K., Kim, H., Lee, J., Song, E.J., Jeong, K.D., Kim, C. and Kim, J. 2013. Fluorescent chemosensor based on bispicolylamine for selective detection of magnesium ions. *Supramol. Chem.*, 25(2): 65-68.
- Kaur, N., Kaur, G., Fegade, U.A., Singh, A., Sahoo, S.K., Kuwar, A.S. and Singh, N. 2017. Anion sensing with chemosensors having multiple NH recognition units. *TrAC Trends Anal. Chem.*, 95: 86-109.
- Khan, M.S., Al-Senaity, A.M., Priyadarshini, M., Shah, A. and Bano, B. 2013. Different conformation of thiol protease inhibitor during amyloid formation: Inhibition by curcumin and quercetin. *J. Fluoresc.*, 23(3): 451-457.
- Khanna, Kanika, Vijay Lakshmi Jamwal, Anket Sharma, Sumit G. Gandhi, Puja Ohri, Renu Bhardwaj, Asma A. Al-Huqail, Manzer H. Siddiqui, Najat Marraiki, and Parvaiz Ahmad. 2019. Evaluation of the role of rhizobacteria in controlling root-knot nematode infection

- in *Lycopersicon esculentum* plants by modulation in the secondary metabolite profiles. *AoB Plants*, 11(6): 69.
- Khanra, S., Ta, S., Ghosh, M., Chatterjee, S. and Das, D. 2019. Subtle structural variation in azine/imine derivatives controls Zn²⁺ sensitivity: ES IPT-CHEF combination for nano-molar detection of Zn²⁺ with DFT support. *RSC Adv.*, 9(37): 21302-21310.
- Kolate, S., Patil, N., Phalak, R., Waghulde, G.P., Patil, C.J., Dhake, R.B. and Fegade, U. 2020. Colorimetric "off-on" probe for Cu²⁺ nanomolar detection in aqueous solution. *J. Adv. Sci. Res.*, 11: 112-136.
- Kumar, G.G.V., Kesavan, M.P., Tamilselvi, A., Rajagopal, G., Raja, J. D., Sakthipandi, K., Rajesh, J. and Sivaraman, G. 2018. A reversible fluorescent chemosensor for the rapid detection of Hg²⁺ in an aqueous solution: It is logic gates behavior. *Sensors Actuat. B Chem.*, 273: 305-315.
- Kuwar, A., Fegade, U., Tayade, K., Patil, U., Puschmann, H., Gite, V., Dalal, D. and Bendre, R. 2013. Bis(2-Hydroxy-3-Isopropyl-6-Methyl-Benzaldehyde) ethylenediamine: A novel cation sensor. *J. Fluoresc.*, 23: 859-864.
- Lehn, J.M. 1995. *Supramolecular Chemistry*. Wiley and Sons, NJ.
- Li, S., Cao, D., Hu, Z., Li, Z., Meng, X., Han, X. and Ma, W. 2019. A chemosensor with a paddle structure based on a BODIPY chromophore for sequential recognition of Cu²⁺ and HSO₃⁻. *RSC Adv.*, 9(59): 34652-34657.
- Maniyazagan, M., Mariadasse, R., Jeyakanthan, J., Lokanath, N.K., Naveen, S., Premkumar, K., Muthuraja, P., Manisankar, P. and Stalin, T. 2017. Rhodamine-based "turn-on" molecular switch FRET-sensor for cadmium and sulfide ions and live cell imaging study. *Sensors Actuat. B Chem.*, 238: 565-577.
- Mao, X., Su, H., Tian, D., Li, H. and Yang, R. 2013. Bipyrene-functionalized graphene as a "Turn-On" fluorescence sensor for manganese (II) ions in living cells. *ACS Appl. Mater. Interfaces*, 5(3): 592-597.
- Meng, X., Cao, D., Hu, Z., Han, X., Li, Z. and Ma, W. 2018. A highly sensitive and selective chemosensor for Pb²⁺ based on quinoline-coumarin. *RSC Adv.*, 8(59), pp.33947-33951.
- Naha, S., Wu, S.P. and Velmathi, S. 2020. Naphthalimide-based smart sensor for CN⁻/Fe³⁺ and H₂S. Synthesis and application in RAW264. 7 cells and zebrafish imaging. *RSC Adv.*, 10(15): 8751-8759.
- Panunzi, B., Diana, R., Concilio, S., Sessa, L., Tuzi, A., Piotto, S. and Caruso, U. 2019. Fluorescence pH-dependent sensing of Zn (II) by a tripodal ligand. A comparative X-ray and DFT study. *J. Luminesc.*, 212: 200-206.
- Park, G.J., Na, Y.J., Jo, H.Y., Lee, S.A. and Kim, C. 2014. A colorimetric organic chemo-sensor for Co²⁺ in a fully aqueous environment. *Dalton Trans.*, 43(18): 6618-6622.
- Patil, N., Dhake, R.B., Fegade, U., Gokulakrishnan, K., Ramalingan, C., Inamuddin, Altalhi, T. and Kanchi, S. 2021. N⁻-(4-(diethylamino)-2-hydroxybenzylidene) isonicotinohydrazide based chemosensor for nanomolar detection of Ni (II) ion. *Int. J. Environ. Anal. Chem.*, 10: 1-17.
- Patil, N.S., Dhake, R.B., Ahamed, M.I. and Fegade, U. 2020. A mini-review on organic chemosensors for cation recognition (2013-19). *J. Fluoresc.*, 30(6): 1295-1330.
- Patil, R., Fegade, U., Kaur, R., Sahoo, S.K., Singh, N. and Kuwar, A. 2015. Highly sensitive and selective determination of Hg²⁺ by using 3-(2-(1H-benzo [d] imidazol-2-yl) phenylimino) methyl) benzene-1, 2-diol as fluorescent chemosensor and its application in the real water sample. *Supramol. Chem.*, 27(7-8): 527-532.
- Patil, S., Fegade, U., Sahoo, S.K., Singh, A., Marek, J., Singh, N., Bendre, R. and Kuwar, A. 2014. Highly sensitive ratiometric chemosensor for selective naked-eye nanomolar detection of Co²⁺ in semi-aqueous media. *Chem. Phys. Chem.*, 15(11): 2230-2235.
- Patil, S., Patil, R., Fegade, U., Bondhopadhyay, B., Pete, U., Sahoo, S.K., Singh, N., Basu, A., Bendre, R. and Kuwar, A. 2015. A novel phthalazine based highly selective chromogenic and fluorogenic chemosensor for Co²⁺ in semi-aqueous medium: application in cancer cell imaging. *Photochem. Photobiol. Sci.*, 14(2): 439-443.
- Pawar, S., Fegade, U., Bhardwaj, V.K., Singh, N., Bendre, R. and Kuwar, A. 2015. 2-((E)-(2-aminophenylimino) methyl)-6-isopropyl-3-methylphenol based fluorescent receptor for dual Ni²⁺ and Cu²⁺ recognition: Nanomol. Detect. *Polyhed.*, 87: 79-85.
- Pendin, D., Norante, R., De Nadai, A., Gherardi, G., Vajente, N., Basso, E., Kaludercic, N., Mammucari, C., Paradisi, C., Pozzan, T. and Mattarei, A. 2019. A synthetic fluorescent mitochondria-targeted sensor for ratiometric imaging of calcium in live cells. *Angewan. Chem.*, 131(29): 10022-10027.
- Sargenti, A., Farruggia, G., Malucelli, E., Cappadone, C., Merolle, L., Marraccini, C., Andreani, G., Prodi, L., Zaccheroni, N., Sgarzi, M. and Trombini, C. 2014. A novel fluorescent chemosensor allows the assessment of intracellular total magnesium in small samples. *Analyst*, 139(5): 1201-1207.
- Scatchard, G.D. 1949. The attractions of proteins for small molecules and ions. *Ann. NY Acad. Sci.*, 51: 660-672.
- Swami, S., Agarwala, A., Behera, D. and Shrivastava, R. 2018. Diaminomaleonitrile-based chromo-fluorescent receptor molecule for selective sensing of Mn (II) and Zn (II) ions. *Sensors Actuat. B Chem.*, 260: 1012-1017.
- Tayade, K., Bondhopadhyay, B., Sharma, H., Basu, A., Gite, V., Attarde, S., Singh, N. and Kuwar, A., 2014. "Turn-on" fluorescent chemosensor for zinc (ii) dipodal ratiometric receptor: application in live cell imaging. *Photochemical & Photobiological Sciences*, 13(7): 1052-1057.
- Xu, J., Yang, Y., Baigude, H. and Zhao, H. 2019. New ferrocene-triazole derivatives for multisignaling detection of Cu²⁺ in aqueous medium and their antibacterial activity. *Spectrochim. Acta Part A Mol. Biomol. Spectrosc.*, 229: 117880.
- Xu, K., Li, Y., Si, Y., He, Y., Ma, J., He, J., Hou, H. and Li, K. 2018. A "turn-on" fluorescent chemosensor for the detection of Hg (II) in buffer-free aqueous solution with excellent selectivity. *J. Luminesc.*, 204: 182-188.
- Yan, R., Wang, Z., Du, Z., Wang, H., Cheng, X. and Xiong, J. 2018. A biomimetic fluorescent chemosensor for highly sensitive zinc (II) detection and its application for cell imaging. *RSC Adv.*, 8(58): 33361-33367.
- Yang, M., Chae, J.B., Kim, C. and Harrison, R.G. 2019. A visible chemosensor based on carbonylhydrazide for Fe (II), Co (II), and Cu (II) in an aqueous solution. *Photochem. Photobiol. Sci.*, 18(5): 1249-1258.
- Yang, X., Wang, Y., Liu, R., Zhang, Y., Tang, J., Yang, E.B., Zhang, D., Zhao, Y. and Ye, Y. 2019. A novel ICT-based two-photon and NIR fluorescent probe for labile Fe²⁺ detection and cell imaging in living cells. *Sensors Actuat. B Chem.*, 288: 217-224.
- Zhang, Q., Ma, R., Li, Z. and Liu, Z. 2020. A multi-responsive crown ether-based colorimetric/fluorescent chemosensor for highly selective detection of Al³⁺, Cu²⁺ and Mg²⁺. *Spectrochim. Acta Part A Mol. Biomol. Spectrosc.*, 228: 117857.
- Zhang, Y., Li, H., Gao, W. and Pu, S. 2019a. Dual recognition of Al³⁺ and Zn²⁺ ions by a novel probe based on diarylethene and its application. *RSC Adv.*, 9(47): 27476-27483.
- Zhang, Y., Zhang, C., Wu, Y., Zhao, B., Wang, L. and Song, B. 2019b. A novel water-soluble naked-eye probe with a large Stokes shift for selective optical sensing of Hg²⁺ and its application in water samples and living cells. *RSC Adv.*, 9(40): 23382-23389.
- Zhao, B., Xu, Y., Fang, Y., Wang, L. and Deng, Q. 2015. Synthesis and fluorescence properties of phenanthrene [9, 10-d] imidazole derivative for Ag⁺ in aqueous media. *Tetrahed. Lett.*, 56(19): 2460-2465.
- Zhou, J.R., Liu, D.P., He, Y., Kong, X.J., Zhang, Z.M., Ren, Y.P., Long, L.S., Huang, R.B. and Zheng, L.S. 2014. A highly selective colorimetric chemosensor for cobalt (II) ions based on a tripodal amide ligand. *Dalton Trans.*, 43(30): 11579-11586.